Langmuir
Article
pubs.acs.org/Langmuir

Adsorption and Aggregation Characteristics of Silver Nanoparticles onto a Poly(4-vinylpyridine) Film: A Comparison with Gold Nanoparticles

Kwan Kim,*[,†] Hyunwoo Ryoo,[†] and Kuan Soo Shin*[,‡]

[†]*Department of Chemistry, Seoul National University, Seoul 151-742, Korea, and* [‡]*Department of Chemistry, Soongsil University, Seoul 156-743, Korea*

Received February 12, 2010. Revised Manuscript Received March 6, 2010

The adsorption and aggregation processes of Ag nanoparticles versus Au nanoparticles onto a poly(4-vinylpyridine) (P4VP) surface has been investigated by means of quartz crystal microbalance (QCM), atomic force microscopy (AFM), and Raman scattering spectroscopy. Both the QCM and AFM data indicated that the citrate-reduced Ag and Au nanoparticles are adsorbed onto P4VP, forming only ~30% and ~17% of surface coverage, respectively, even after 6 h of adsorption in solution. The P4VP film was too thin to observe its normal Raman spectrum, but the Raman peaks of P4VP could be detected upon the adsorption of Ag (or Au) nanoparticles onto the film, due to the surface-enhanced Raman scattering (SERS) effect associated with the localized surface plasmon of Ag (or Au) nanoparticles. When in contact with the solution of Ag (or Au) nanoparticles, the SERS peaks of P4VP thus increased linearly as a function of time, in a manner similar to that shown by the QCM and AFM data. In the interim, however, as the sol solution was drained, the SERS signal of P4VP was intensified about twice probably due to the aggregation of nanoparticles. Eventually, the SERS signal derived from the Ag nanoparticles became two times stronger than that from the same number of Au nanoparticles, at least under the 632.8 nm excitation, suggesting that Ag nanoparticles must be more advantageous than Au nanoparticles in elucidating by SERS the physicochemical characteristics of organic/polymeric surfaces and suggesting their likely advantages in metallic staining in immunoassays.

Introduction

Noble metal nanoparticles such as gold and silver exhibit interesting optical phenomena in the visible wavelength range.[1,2] When they are assembled into a close-packed structure, the optical properties change dramatically due to the interaction of the particles' local electric fields.[3] Au and Ag nanostructures in 2-D and 3-D architectures are, therefore, attractive especially in the development of optical and biomedical devices.[4−9] For this reason, a variety of methods have been proposed for the preparation of uniform films of nanoparticles,[10,11] the most effective and environmentally benign of which is supposed to be self-assembly conducted in a solution phase.[12−15]

The assembly of nanoparticles in terms of alignment, interparticle separation, and stability is an important task in the development of nanodevices. A key issue therein is to understand the self-assembly process itself. The adsorption kinetics of metal nanoparticles onto a solid substrate in a solution phase is, however, governed by numerous factors including the physicochemical characteristics of the nanoparticles and the solid substrates.[16,17] Although the number of nanoparticles being adsorbed onto a solid substrate may be monitored in situ by means of a quartz crystal microbalance (QCM), the arrangement of nanoparticles is usually identified afterward by taking scanning electron microscopy (SEM) or atomic force microscopy (AFM) images. It is certainly desirable to get information on the status of nanoparticles in real time scales. Recently, Enders et al.[18] demonstrated that in situ surface-enhanced infrared absorption (SEIRA) spectroscopy can be used to examine the adsorption and desorption of Au nanoparticles on an amine-derivatized SiO_2/Si surface.

Very recently, we reported that the adsorption and aggregation processes of Au nanoparticles on a proper polymer surface can be monitored by surface-enhanced Raman scattering (SERS) spectroscopy.[19] This is possible because SERS is highly active with Au nanoaggregates. Specifically, we were able to analyze the adsorption process of citrate-reduced Au nanoparticles onto a film of poly(4-vinylpyridine) (P4VP). In order to help analyze the SERS spectra, we separately conducted QCM, UV/vis spectroscopy,

*Corresponding authors. Telephone: +82-2-8806651 (K.K.); +82-2-8200436 (K.S.S.). Fax: +82-2-8891568 (K.K.); +82-2-8244383 (K.S.S.). E-mail: kwankim@snu.ac.kr (K.K.); kshin@ssu.ac.kr (K.S.S.).

(1) Jain, P. K.; Huang, X.; El-Sayed, I. H.; El-Sayed, M. A. *Plasmonics* **2007**, *2*, 107.
(2) Daniel, M.-C.; Astruc, D. *Chem. Rev*. **2004**, *104*, 293.
(3) Míguez., H.; López, C.; Meseguer, F.; Blanco, A.; Vázquez, L.; Mayoral, R.; Ocaña, M.; Fornés, V.; Mifsud, A. *Appl. Phys. Lett*. **1997**, *71*, 1148.
(4) Abdelsalam, M. E.; Bartlett, P. N.; Baumberg, J. J.; Cintra, S.; Kelf, T. A.; Russell, A. E. *Electrochem. Commun*. **2005**, *7*, 740.
(5) Nykypanchuk, D.; Maye1, M. M.; Lelie, D. V. D.; Gang., O. *Nature* **2008**, *451*, 549.
(6) Lu, L.; Randjelovic, I.; Capek, R.; Gaponik, N.; Yang, J.; Zhang, H.; Eychmüller, A. *Chem. Mater*. **2005**, *17*, 5731.
(7) Lombardia, I.; Cavallottic, P. L.; Carraro, C.; Maboudian, R. *Sensors Actuat. B-Chem* **2007**, *125*, 353.
(8) Kubo, S.; Gu, Z.-Z.; Tryk, D. A.; Ohko, Y.; Sato, O.; Fujishima, A. *Langmuir* **2002**, *18*, 5043.
(9) Tan, R. Z.; Agarwal, A.; Balasubramanian, N.; Kwong, D. L.; Jiang, Y.; Widjaja, E.; Garland, M. *Sens. Actuators, A: Phys* **2007**, *139*, 36.
(10) Sokolov, K.; Chumanov, G.; Cotton, T. M. *Anal. Chem*. **1998**, *70*, 3898.
(11) Liu, Y.; Wang, Y.; Claus, R. O. *Chem. Phys. Lett*. **1998**, *298*, 315.
(12) Musick, M. D.; Keating, C. D.; Lyon, L. A.; Botsko, S. L.; Peña, D. J.; Holliway, W. D.; McEvoy, T. M.; Richardson, J. N.; Natan, M. J. *Chem. Mater*. **2000**, *12*, 2869.
(13) Zhang, F.; Srinivasan, M. P. *Langmuir* **2007**, *23*, 10102.
(14) Jiang, Y.; Shen, Y.; Wu, P. *J. Colloid Interface Sci*. **2008**, *319*, 398.
(15) Freeman, R. G.; Grabar, K. C.; Allison, K. J.; Bright, R. M.; Davis, J. A.; Guthrie, A. P.; Hommer, M. B.; Jackson, M. A.; Smith, P. C.; Walter, D. G.; Natan, M. J. *Science* **1995**, *267*, 1629.
(16) Park, S.-H.; Im, J.-H.; Im, J.-W.; Chun, B.-H.; Kim, J.-H. *Microchem. J*. **1999**, *63*, 71.
(17) Bright, R. M.; Musick, M. D.; Natan, M. J. *Langmuir* **1998**, *14*, 5695.
(18) Enders, D.; Nagao, T.; Nakayama, T.; Aono, M. *Langmuir* **2007**, *23*, 6119.
(19) Kim, K.; Ryoo, H.; Lee, Y. M.; Shin, K. S. *J. Colloid Interface Sci*. **2010**, *342*, 479.

and AFM measurements. The QCM data was in fair agreement with the AFM data, suggesting that the number of Au nanoparticles adsorbed onto P4VP increased almost linearly with time. However, the UV/vis absorbance at ~650 nm, associated with Au nanoaggregates, increased more rapidly at longer immersion times compared with the QCM and AFM data. The UV/vis absorbance in turn correlated fairly well with the SERS observation, suggesting that the SERS signal should be very susceptible to the aggregation of Au nanoparticles.

In this work, we have investigated the adsorption and aggregation characteristics of Ag nanoparitcles on a P4VP film. The purpose of this work is to identify any similarities and/or dissimilarities in the adsorption behaviors of Au and Ag nanoparticles on a polymeric surface. We found on the one hand that citrate-reduced Ag nanoparticles were adsorbed onto the P4VP film twice as rapidly as citrate-reduced Au nanoparticles in solution. On the other hand, the Raman signal of P4VP was found to intensify by a factor of 2 when the wet film was dried off, definitely due to the formation of Ag or Au nanoaggregates in air, resulting eventually in the Raman signal derived from the Ag nanoparticles becoming about two times more intense than that derived from the same number of Au nanoparticles. This information is very valuable, particularly because the adsorption of Ag or Au nanoparticles onto biological substrates is deeply associated with the metal staining that is widely used in immunoassays and biomolecular sensing.[20−22]

Experimental Section

Silver nitrate ($AgNO_3$), hydrogen aurate ($HAuCl_4$), sodium citrate, and P4VP (MW ~160 kDa) were purchased from Aldrich, and used as received. Other chemicals, unless specified, were reagent-grade, and highly purified water, with a resistivity greater than 18.0 MΩ·cm (Millipore Milli-Q System), was used in preparing aqueous solutions. Ag and Au sols were prepared by following the recipes of Lee and Meisel.[23] Initially, 100 mL of $AgNO_3$ solution (0.75 mM) was brought to the boil. Subsequently, 1% (w/v) sodium citrate (9 mL) was added therein under vigorous stirring, and boiling was continued for 30 min. For Au sol, 100 mL of $HAuCl_4$ (0.75 mM) solution and 4 mL of 1% (w/v) sodium citrate were used to obtain Au nanoparticles with sizes comparable to those of Ag nanoparticles. When conducting the adsorption experiment, these sols were diluted twice with water.

Glass slides and capillaries, silicon wafers, as well as Au-coated quartz electrodes, used as substrates to support the films of P4VP, were cleaned by soaking in a piranha solution. Caution! *Piranha solution is very energetic and requires care in handling as it reacts violently with organic compounds*. The cleaned substrates were dipped in a 0.4 M ethanolic solution of P4VP for 30 min, and then withdrawn vertically and washed with ethanol; when coating P4VP onto the inside surface of a glass capillary, the solution injected into the capillary was withdrawn after 30 min using a syringe.

The ζ potential of Ag and Au nanoparticles was measured in a Malvern Zetasizer 3000HS (Malvern Instruments, UK). UV/vis spectra were obtained with a SINCO S-2130 UV/vis absorption spectrometer. Transmission electron microscopy (TEM) images were taken on a JEM-200CX transmission electron microscope at 200 kV. The thickness of P4VP films was estimated using a Rudolph Auto EL II optical ellipsometer. AFM images were obtained using a Digital Instrument model Nanoscope IIIa scanning probe microscope.

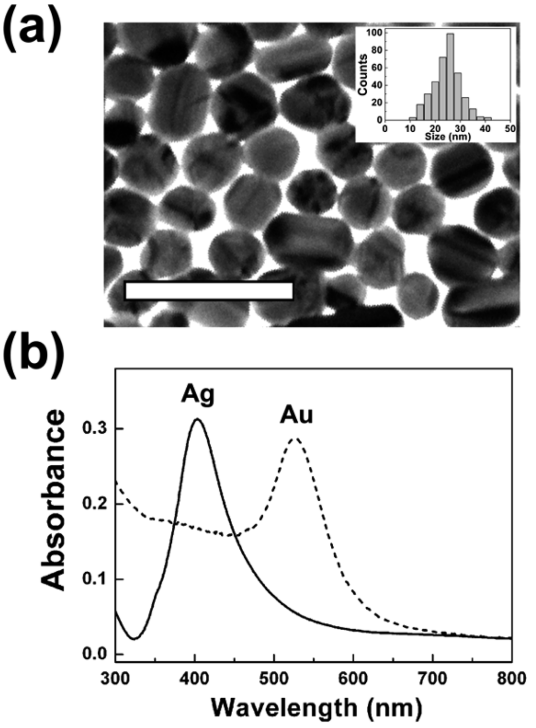

Figure 1. (a) Typical TEM image (scale bar = 100 nm). The inset of part a shows a histogram of the particle size distribution of Ag nanoparticles. (b) UV/vis absorption spectra of Ag and Au citrate sols.

A QCM experiment was conducted using an Au-coated, AT-cut quartz crystal (fundamental resonance frequency, f_o = 10 MHz): the apparent area of the electrode was 0.20 cm^2.[24] A P4VP-coated Au electrode was fixed onto a crystal holder using a conductive adhesive, and then the holder was fastened onto the QCM cell through the Kalez O-rings. First, pure water was added into the QCM cell, and left to stabilize. Ag (or Au) sol was subsequently injected into the cell, with an equal volume to the water added beforehand, and then the frequency change was monitored as a function of time.

Raman spectra were obtained by using a Renishaw Raman system model 2000 spectrometer equipped with an integral microscope (Olympus BH2-UMA). The 632.8 nm line from a 17 mW He/Ne laser (Spectra Physics model 127) was used as the excitation source: the typical laser power at the sampling position was 0.2 mW. When measuring the Raman spectra of P4VP under in situ conditions, Ag or Au sol was made to flow through a P4VP-coated capillary by means of a Sage Instruments Model 341 syringe pump.

Two-dimensional finite-difference time-domain (2D-FDTD)[25] electrodynamics simulation was carried out for silver and gold nanoparticles using a FDTD solutions software provided by Lumerical Solutions, Inc.

Results and Discussion

We confirmed in our previous work that the P4VP film prepared by dip coating at 0.4 M of P4VP in ethanol is very robust in an aqueous electrolytic solution.[19] The ellipsometric thickness of ~80 nm remained constant even after soaking for 10 h in an aqueous electrolytic solution of 5 mM $NaNO_3$ and 0.5% sodium citrate: the latter solution was chosen because of its similar characteristics to aqueous Ag and Au sols.

(20) Enders, D.; Rupp, S.; Küller, A.; Pucci, A. *Surf. Sci.* **2006**, *600*, L305.
(21) Han, X. X.; Cai, L. J.; Guo, J.; Wang, C. X.; Ruan, W. D.; Han, W. Y.; Xu, W. Q.; Zhao, B.; Ozaki, Y. *Anal. Chem.* **2008**, *80*, 3020.
(22) Kim, N. H.; Lee, S. J.; Kim, K. *Chem. Commun.* **2003**, *6*, 724.
(23) Lee, P. C.; Meisel, D. *J. Phys. Chem.* **1982**, *86*, 3391.
(24) Ha, T. H.; Kim, C. H.; Park, J. S.; Kim, K. *Langmuir* **2000**, *16*, 871.
(25) Sullivan, D. M. *IEEE Microwave Theory and Techniques Society., Electromagnetic simulation using the FDTD method*; IEEE Press: New York, 2000.

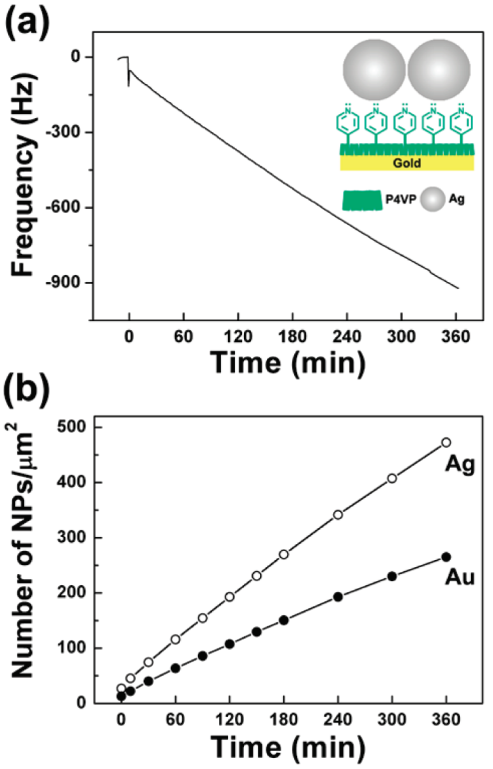

Figure 2. (a) Time response of QCM measured after the addition of Ag sol into a QCM cell containing a P4VP-coated Au electrode. The inset of part a shows the adsorption scheme of Ag nanoparticles onto P4VP film via pyridine N atoms. (b) Number of Ag nanoparticles adsorbed onto P4VP drawn as a function of immersion time as well as the number of Au nanoparticles adsorbed on P4VP under the same conditions.

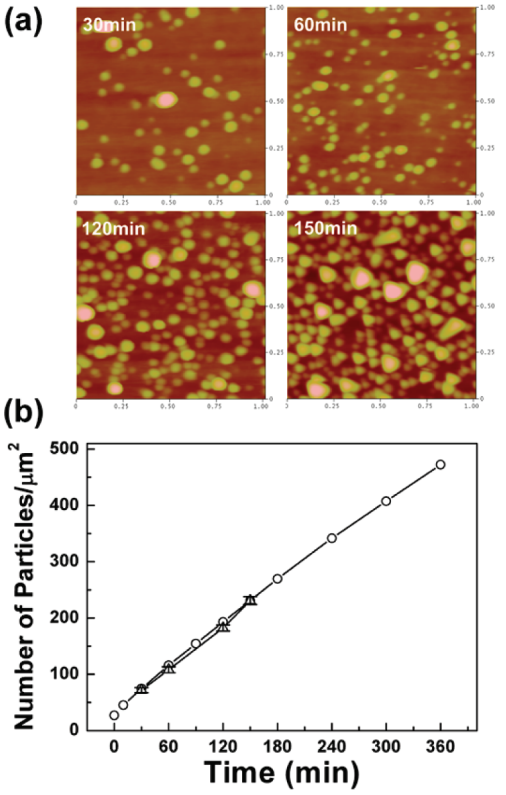

Figure 3. (a) AFM images (1 μm $\times$ 1 μm scales) taken after soaking a P4VP film for certain period of time in Ag sol. (b) Number of Ag nanoparticles (NPs) per 1 μm^2 of P4VP, counted from AFM images (triangles, average at seven different areas) and estimated from QCM data (circles), drawn versus the adsorption time.

Figure 1a shows the TEM image of Ag sol particles. According to the histogram shown as the inset of Figure 1a, the mean diameter of the particles is 24.9 $\pm$ 5.2 nm; as reported previously, the mean diameter of Au nanoparticles is 24.8 $\pm$ 3.9 nm. As shown in Figure 1b, the Ag and Au sols exhibited very distinct surface plasmon absorption bands centered at 405 and 525 nm, respectively. The ζ potential measurements indicated that both the Ag and Au nanoparticles were negatively charged, i.e. -49.3 ± 2.4 and -41.9 ± 1.8 mV, respectively, due to the deprotonation of the citrate moiety.

The surface coverage of P4VP by Ag (or Au) nanoparticles would then be limited owing to the repulsive interaction of the nanoparticles. From the electrostatic point of view, Ag nanoparticles could experience more repulsive interaction than Au nanoparitcles. From the chemical point of view, however, both Ag and Au nanoparticles should nonetheless interact strongly with the pyridine N atoms. This can be inferred from the fact that adding pyridine into Ag and Au sols prepared by the citrate reduction method results in the appearance of SERS peaks of pyridine, caused by the aggregation of Ag(Au) nanoparticles by pyridine and the concomitant adsorption of pyridine onto the Ag(Au) nanoaggregates. It obviously indicates that the adsorption strength of pyridine onto Ag(Au) is greater than that of citrate. On these grounds, we first monitored the adsorption behavior of Ag nanoparticles onto P4VP by QCM.

Figure 2a shows the QCM response. In this measurement, a P4VP-coated electrode was initially allowed to stabilize in water in the QCM cell. As the Ag sol was subsequently added into the water, the QCM frequency dropped within 1 min by as much as 54.0 Hz, and then decreased slowly, but almost linearly with time. The first sharp decrease is due to an initial fast adsorption of Ag nanoparticles onto the surface of the P4VP; the interaction between the pyridine N atoms and the Ag nanoparticles must be energetically favorable. Owing to such chemical interaction, the QCM frequency decreased in total by 918 Hz in 6 h. According to the Sauerbrey equation,[26] the frequency change of 918 Hz corresponds to an adsorption of 472 Ag nanoparticles per 1 μm^2 of P4VP. Figure 2b represents the number of Ag nanoparticles adsorbed onto P4VP drawn as a function of time, taking the average size of Ag nanoparticles (25 nm) into consideration. The number of particles adsorbed over 6 h, i.e. 472, is far smaller than that attainable by close packing of the particles, i.e., 1600 (= 40 $\times$ 40). The surface coverage would be at best ~30%. The repulsive interaction of negatively charged particles must have hindered the formation of a close-packed silver nanoparticle film on the P4VP. For comparison, the number of Au nanoparticles adsorbed onto P4VP under the same conditions is also shown in Figure 2b. In all adsorption experiments, the concentrations of Ag and Au nanoparticles were adjusted to be the same at 1.6 nM. Surprisingly, twice as many Ag particles were adsorbed onto P4VP than Au particles in 6 h. On the basis of the ζ potentials of Au and Ag nanoparticles, Au particles should be adsorbed more favorably onto P4VP, contrary to the observation. This dictates that the adsorption strength of Ag onto the pyridine N atoms is far greater than that of Au. The sparse distribution of Ag and Au nanoparticles was also be confirmed by AFM.

Subsequently, multiple P4VP films on silicon wafers were immersed in Ag sols, and then at certain intervals the

(26) Sauerbrey, G. Z. *Phys.* **1959**, *155*, 206.

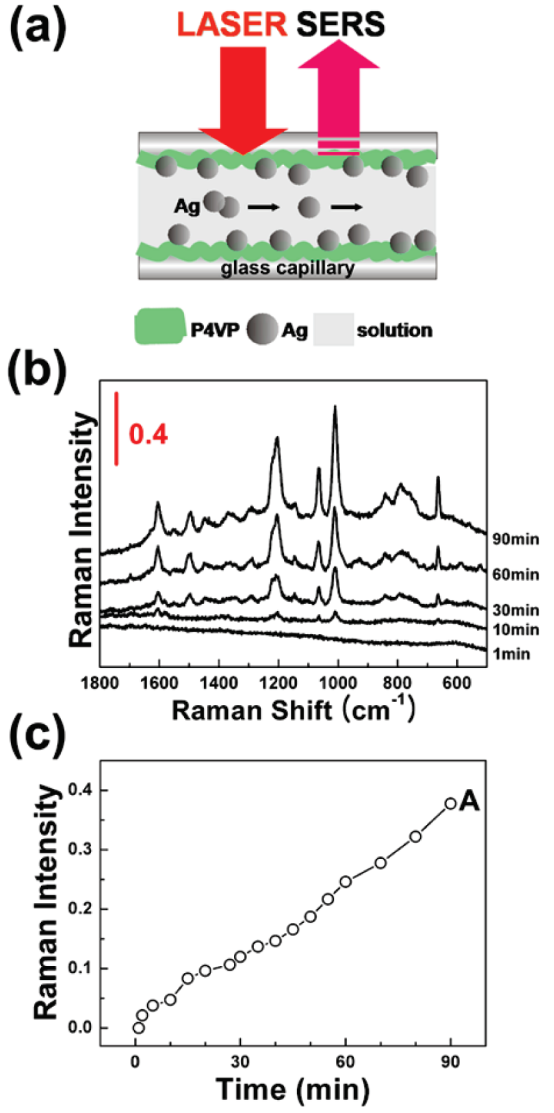

Figure 4. (a) Experimental arrangement for the acquisition of Raman spectra using a P4VP-coated capillary. (b) Series of Raman spectra taken during the flow of Ag sol through a P4VP-coated capillary. (c) Peak intensity of the 9a band of P4VP at 1201 cm^{-1} in part b drawn versus the adsorption time of Ag nanoparticles.

Ag-adsorbed P4VP films were withdrawn, one-by-one, from the sol for up to 2.5 h. Figure 3a shows a series of AFM images for those films: Owing to the tip convolution, the AFM images of Ag nanoparticles are elongated along the scanning direction. In the early stages, there were only rare occasions where two or more Ag nanoparticles were in contact. Close contact occurred more often for a sample dipped longer in Ag sol. In Figure 3b the number density of Ag nanoparticles counted from the AFM images (triangles) is shown: Notice that the error bars representing one standard deviation are smaller than the symbols used. The number densities estimated from the QCM data are also reproduced in Figure 3b (circles). Both densities are seen to be similar. Much the same observation was made when Au nanoparticles were adsorbed onto the P4VP films. As already mentioned, twice as many Ag particles were adsorbed on P4VP than Au particles during a designated period. Hence, the number of Ag nanoparticles adsorbed onto P4VP for 1.5 h, i.e. 154 μm^{-2}, for instance, is comparable to that of Au nanoparticles adsorbed during 3 h, i.e. 151 μm^{-2}.

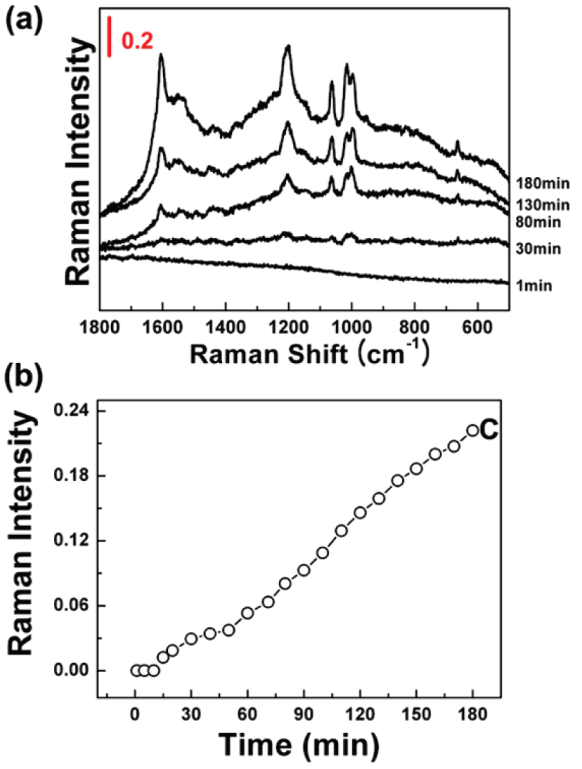

Figure 5. (a) Series of Raman spectra taken during the flow of Au sol through a P4VP-coated capillary. (b) Peak intensity of the 9a band of P4VP at 1201 cm^{-1} in part a drawn versus the adsorption time of Au nanoparticles.

Figure 4b shows a series of Raman spectra taken during the flow of Ag sol through a P4VP-coated glass capillary: their measurement scheme is shown in Figure 4a. The present Raman scattering data are in one-to-one correspondence with the QCM data in Figure 2a. At the beginning, no peak is found since the P4VP film is too thin to be detected by normal Raman scattering. Raman peaks begin to emerge upon the adsorption of Ag nanoparticles, definitely due to the SERS effect.[27,28] All the peaks in Figure 4b can be attributed to Ag adsorbed on P4VP: 1598 cm^{-1} (8a, ring stretch); 1558 cm^{-1} (8b, ring stretch); 1201 cm^{-1} (9a, CH in-plane bend); 1068 cm^{-1} (18a, CH in-plane bend); 1018 cm^{-1} (6); 999 cm^{-1} (1, ring breathing). In Figure 4c is shown the peak intensity of the 9a band at 1201 cm^{-1} drawn versus the adsorption time for Ag nanoparticles adsorbed onto the P4VP film. Much the same intensity variation is observed both from the ν_1 band at 999 cm^{-1} and the ν_6 band at 1018 cm^{-1}. The intensity variation is quite linear, similar to the QCM data in Figure 2a. This is not unexpected since most of the Ag nanoparticles must be positioned separately in such low surface coverage. The number of Ag nanoparticles adsorbed on P4VP for 1.5 h, i.e., 154 μm^{-2}, corresponds merely to the surface coverage of ~9.6%. The Raman signal of P4VP would then be proportional to the number of Ag nanoparticles adsorbed onto the film.

Assuming that both the Ag and Au nanoparticles were perfectly spherical with a mean diameter of 25 nm, the maximum electromagnetic field intensity calculated using 2D-FDTD around an Au nanoparticle is to be 10% higher than that around an Ag nanoparticle under the 632.8 nm radiation. According to the electromagnetic enhancement mechanism, the Raman signal of P4VP should then be 1.2 times stronger under the flow of an Au

(27) Lee, J. J.; Lee, S. J.; Kim, K. *Mol. Cryst. Liq. Cryst.* **2004**, *424*, 1.
(28) Kim, K.; Yoon, J. K. *J. Phys. Chem. B* **2005**, *109*, 20731.

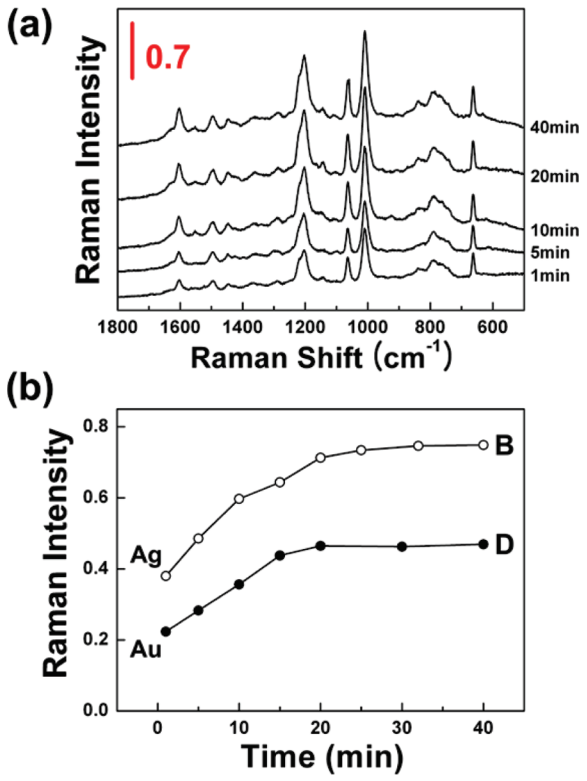

Figure 6. (a) Series of Raman spectra taken timewise in air after the flow of Ag sol for 1.5 h through a P4VP-coated capillary: dry air was forced to flow through the capillary using a syringe pump. (b) (Ag) Peak intensity of the 9a band of P4VP at 1201 cm^{-1} in part a drawn versus the drying time. (Au) Peak intensity of the 9a band of P4VP at 1201 cm^{-1} measured timewise in air after the flow of Au sol for 3 h through a P4VP-coated capillary.

sol than under the flow of an Ag sol. This is in sharp contrast with the observations in Figures 4c and 5b. One possible reason for this discrepancy would be the greater contribution of chemical enhancement by Ag nanoparticles than Au nanoparticles. Otherwise, the discrepancy would have arisen from the different morphologies of Au and Ag nanoparticles.[17,29,30] Although it was difficult to quantify, Ag nanoparticles appeared to be more ellipsoidal than Au nanoparticles in the TEM images. Hence, we assume that the presence of highly irregular Ag nanoparticles including ellipsoids and rods are associated with the discrepancy. According to a 2D-FDTD calculation, the maximum Raman signal of P4VP is 1.8 times stronger at an ellipsoidal Ag nanoparticle with an aspect ratio of 1.35 than at a spherical Ag nanoparticle.

One may certainly expect that Ag nanoparticles adsorbed onto P4VP in solution become aggregated upon the evaporation of water.[31] The Raman signal would then be affected by the agglomeration of Ag nanoparticles. To see the effect, we have measured Raman spectra of the P4VP film under ambient conditions. Figure 6a shows a series of Raman spectra taken timewise in air after draining out the Ag sol following its flowing for 1.5 h through a P4VP-coated capillary. The Raman signal of P4VP has, in fact, increased about twice after drying in air. This is more evident from Figure 6b in which the growth of the 9a band at 1201 cm^{-1} is shown. The intensification of the Raman peaks must be due to the agglomeration of Ag nanoparticles caused by the

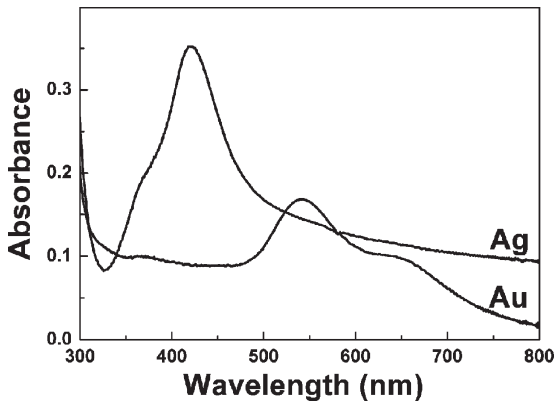

Figure 7. UV/vis absorption spectra taken after a P4VP film was soaked in Ag sol and Au sol for 1.5 and 3 h, respectively.

drying of the P4VP film. The aggregation of Ag nanoparticles would produce "hot" sites for SERS, and some pyridine moieties located inside or near the "hot" sites could then show significantly enhanced Raman scattering.

A dramatic increase in Raman signal is also observed when an Au nanoparticle-adsorbed P4VP film is dried off. In Figure 6b the growth of the 9a band of P4VP measured timewise after draining out the Au sol is also shown. Once again, the Raman signal has increased by a factor of 2 upon drying out the P4VP film. It should be remembered that the number of Au nanoparticles present on P4VP at point D in Figure 6b is comparable to that of the Ag nanoparticles on P4VP at point B in Figure 6b. The Raman signal at point B is ~1.6 times stronger than that at point D. Associated with this, we show in Figure 7 the UV/vis absorption spectra of a P4VP film taken in air after soaking in an Ag sol for 1.5 h and in an Au sol for 3 h: the number of Ag and Au nanoparticles adsorbed on P4VP should be comparable to each other under those conditions. It is seen that the absorbance at 632 nm is stronger for a P4VP film soaked in Ag sol than that in Au sol. This is in conformity with the greater SERS peaks of P4VP induced by Ag nanoparticles than by Au nanoparticles in Figure 6b.

Conclusion

In this work, we have examined the adsorption of citrate-reduced Ag nanoparticles onto P4VP, using QCM, AFM, and Raman spectroscopy. The QCM data was in fair agreement with that of AFM, both of which suggested that the number of Ag nanoparticles adsorbed onto P4VP increased almost linearly with time. The surface coverage of Ag nanoparticles on P4VP was only ~30% even after 6 h of adsorption in solution, however, supposedly due to the repulsive interaction of the Ag nanoparticles. The surface coverage of Ag nanoparticles is nonetheless twice that of Au nanoparticles under the same conditions, suggesting that the adsorption strength of Ag to the pyridine N atoms must be far greater than that of Au to the pyridine. Raman peaks of P4VP could be identified by means of the SERS effect of Ag nanoparticles. When in contact with Ag sol, the Raman peak of P4VP increased linearly as a function of time, as similarly shown by the QCM and AFM data, but the Raman signal was further increased by a factor of 2 upon drying out the P4VP film, suggesting that the aggregation of Ag nanoparticles must have occurred upon drying in air. A similar observation was made using Au nanoparticles. The Raman signal of P4VP induced by Ag nanoaggregates in air was approximately two times more intense than that induced by Au nanoaggregates. Supposedly, then, Ag nanoparticles

(29) Xu, H.; Aizpurua, J.; Käll, M.; Apell, P. *Phys. Rev. E* **2000**, *62*, 4318.
(30) Frens, G. *Nature Phys. Sci.* **1973**, *241*, 20.
(31) Malynych, S.; Luzinov, I.; Chumanov, G. *J. Phys. Chem. B* **2002**, *106*, 1280.

must be more advantageous than Au nanoparticles, at least when they were produced by the citrate reduction method, in elucidating by SERS the physicochemical characteristics of organic/polymeric surfaces, including the metal staining in immunoassays and biomolecular sensing.

Acknowledgment. This work was supported by National Research Foundation of Korea Grant funded by the Korean Government (Grant R11-2007-012-02002-0, M10703001067-08M0300-06711-Nano2007-02943, KRF-2008-313-C00390, and 2009-0072467).